

# Clinical Applications of Magnetic Resonance Imaging—Current Status

DRISS CAMMOUN, MD, *Denver*; WILLIAM R. HENDEE, PhD, *Chicago*, and KATHLEEN A. DAVIS, MD, *Denver*

*Magnetic resonance imaging has far-reaching real and possible clinical applications. Its usefulness has been best explored and realized in the central nervous system, especially the posterior fossa and brain stem, where most abnormalities are better identified than with computed tomography. Its lack of ionizing radiation and extreme sensitivity to normal and abnormal patterns of myelination make magnetic resonance imaging advantageous for diagnosing many neonatal and pediatric abnormalities. New, reliable cardiac gating techniques open the way for promising studies of cardiac anatomy and function. The ability to image directly in three orthogonal planes gives us new insight into staging and follow-up of pelvic tumors and other pelvic abnormalities. Exquisite soft tissue contrast, far above that attainable by other imaging modalities, has made possible the early diagnosis of traumatic ligamentous knee injury, avascular necrosis of the hip and diagnosis, treatment planning and follow-up of musculoskeletal neoplasms.*

(Cammoun D, Hendee WR, Davis KA: Clinical applications of magnetic resonance imaging—Current status, *In* High-tech medicine [Special Issue]. West J Med 1985 Dec; 143:793-803)

**M**agnetic resonance (MR) imaging has the potential to portray normal anatomy and to show abnormal conditions in many of the body's organ systems and anatomic regions. In this article we examine the current realization of this potential for several regions and organ systems, including the central nervous system (CNS), head, neck, mediastinum and chest, cardiovascular system, breast, abdomen, pelvis and musculoskeletal system.

### Central Nervous System

Many studies have confirmed the ability of MR imaging to show abnormalities in the entire central nervous system, including the brain, the brain stem and the spinal cord. This ability has caused some imaging physicians to identify MR imaging as the preferred imaging modality for many CNS diseases. Although other specialists have been a bit more cautious, there is little question that MR imaging will be extremely valuable in diagnosing a wide spectrum of CNS disorders.

#### Posterior Fossa

Magnetic resonance imaging is an ideal tool to explore the posterior fossa. It provides exquisite contrast sensitivity and is not impeded by the thickness of the skull in this region (Figure 1). Sagittal views are particularly useful for posterior fossa studies.

Low-grade lesions in the posterior fossa, including brain-stem tumors, are detected more reliably with MR imaging than with computed tomography (CT).<sup>1-3</sup> MR imaging is an accurate method for detecting masses in the cerebellopontine angle and is a noninvasive alternative to contrast-enhanced CT and air cisternography in diagnosing acoustic neuroma.<sup>4</sup> In part, these advantages are due to the absence of signal from the petrous bone.

#### Brain Tumors

Magnetic resonance imaging appears to be the preferred modality for investigating many brain tumors, primarily because many—but not all—tumors have increased spin-lattice (T1) and spin-spin (T2) relaxation times. Small meningiomas can be missed because of their variable T2 relaxation time; the use of gadolinium (Gd)-diethylenetriaminepentaacetic acid (DTPA) as a contrast agent for MR imaging seems to improve the detection of meningiomas.<sup>5</sup> Compared with adjacent normal brain tissue, meningiomas are often hypointense—that is, dark when a spin-echo pulse sequence is used with a short repetition time. At other times a meningioma has a characteristic thin hypointense rim that delineates the tumor.<sup>5</sup> Separation of tumor from surrounding edema has been possible in several instances.<sup>3</sup> However, MR imaging produces results superior to those of CT only if a clinician knows which pulse sequence to use and how to select the pulse vari-

From AMC Cancer Research Center and the Division of Radiological Sciences, Department of Radiology, University of Colorado Health Sciences Center, Denver. Dr Hendee is now Assistant Vice-President for Science and Technology, American Medical Association, Chicago.

Reprint requests to Kathleen A. Davis, MD, Department of Radiology, A034, University of Colorado Health Sciences Center, 4200 E 9th Ave, Denver, CO 80262.

## ABBREVIATIONS USED IN TEXT

CNS = central nervous system  
 CSF = cerebrospinal fluid  
 CT = computed tomography  
 Gd-DTPA = gadolinium-diethylenetriaminepentaacetic acid  
 MR = magnetic resonance  
 T1 = spin-lattice relaxation time  
 T2 = spin-spin relaxation time

ables within that sequence. Obviously, this statement is true not only for the detection of brain tumors but for lesions in general.

In patients with neurofibromatosis, MR imaging is useful in delineating lesions such as optic gliomas, bilateral acoustic neuromas, meningiomas, infiltrating gliomas and hamartomas. It may also prove useful in determining which neurofibromas have progressed to neurofibrosarcoma.<sup>6</sup>

*Inflammatory Disease*

Multiple sclerosis is the most disabling neurologic disease to strike young adults.<sup>7</sup> Early diagnosis of multiple sclerosis is difficult to establish, and the disease is often unrecognizable at an early stage on CT images. MR imaging is a much more sensitive technique than CT for detecting chronic plaques of multiple sclerosis, even when the standard examination is a delayed double-dose-enhanced CT scan.<sup>7</sup> In the acute phase, MR imaging and CT appear to have about equal sensitivity.

Multiple sclerosis lesions have prolonged T1 and T2 relaxation times and are observed in periventricular deep white matter as well as in the cerebellum, brain stem and spinal cord. Multiple sclerosis plaques can also be seen at the junction of grey and white matter and in grey matter. If there is no

clinical evidence of multiple sclerosis, these findings suggest additional differential diagnoses, such as multiple infarcts within the deep white matter, Binswanger's disease (subcortical atherosclerotic encephalopathy), vasculitis, early metastases without mass effect or edema, progressive multifocal leukoencephalopathy, encephalitis and normal aging. Sometimes large or confluent multiple sclerosis plaques resemble metastases with mass effect and edema.

Focal lesions have been found by MR imaging in eight patients with systemic lupus erythematosus and the recent onset of neuropsychiatric symptoms. Corresponding CT findings were visible in only two of seven of these patients.<sup>8</sup>

*Trauma*

Magnetic resonance imaging is very sensitive to parenchymal cerebral contusions and small subdural hematomas. Gandy and co-workers found MR imaging helpful when standard skull radiography and CT showed no evidence of these conditions.<sup>9</sup> Acute subarachnoid and intracerebral hemorrhage undergoes three temporal phases. In the acute phases (for about three days), T1 and T2 times are relatively long. In the subacute phase (approximately three days to two weeks), the T1 time shortens, producing a strong signal on T1-weighted scans. This phenomenon is thought to be due to oxidative denaturation of hemoglobin, resulting in the formation of methemoglobin, a strongly paramagnetic substance that shortens the T1 relaxation time.<sup>10,11</sup> After about two weeks, as methemoglobin is resorbed, the T1 time lengthens. When blood collections are in the isodense phase in CT, MR imaging can be very helpful in establishing the diagnosis (Figure 2).



**Figure 1.**—**Left**, spin echo techniques (echo time, 30 ms; repetition time, 600 ms. Sagittal view through the midline of the brain showing extension of a cystic astrocytoma involving the medulla and upper cervical cord. **Right**, A computed tomographic scan through the posterior fossa of the same patient shows a hypodense area blurred by streak artifact as a result of the thickness of the skull in this region.

*Vascular Disease*

In both subacute and acute phases, infarcted brain tissue is characterized by increased T1 and T2 times. The infarcted area has sharp margins and yields an intense signal in T2-weighted images and a weak signal in T1-weighted images.<sup>12</sup> After a few days, a hemorrhagic infarct yields an intense

signal in T1-weighted scans because of the presence of blood. In the chronic phase, infarcts have two distinct appearances: either a central area of low signal intensity with a peripheral zone of higher intensity, or as an area of cerebrospinal fluid (CSF) intensity without a peripheral zone of higher intensity.<sup>12</sup>

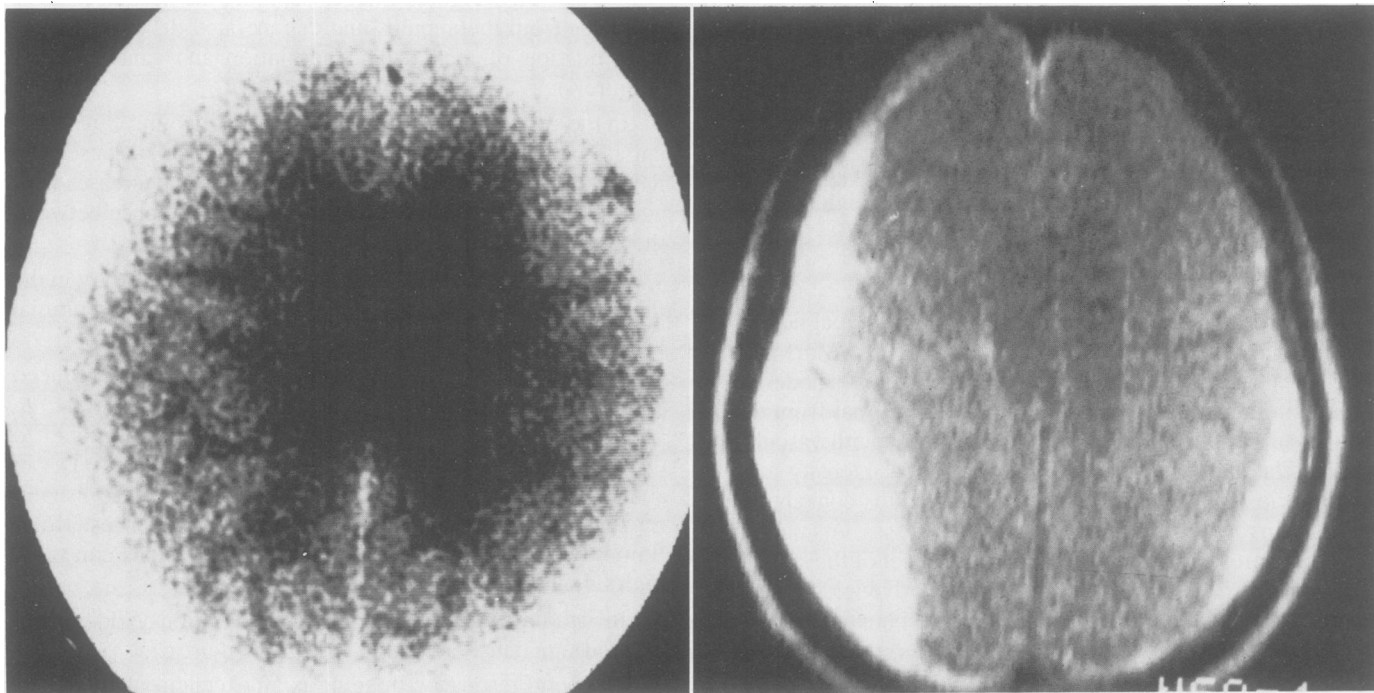


**Figure 2.**—Left, A bilateral subdural hematoma is not visible on a computed tomographic scan as its density is similar to that of brain tissue. Right, The bilateral hematoma is depicted better on magnetic resonance imaging with a long spin-echo sequence.

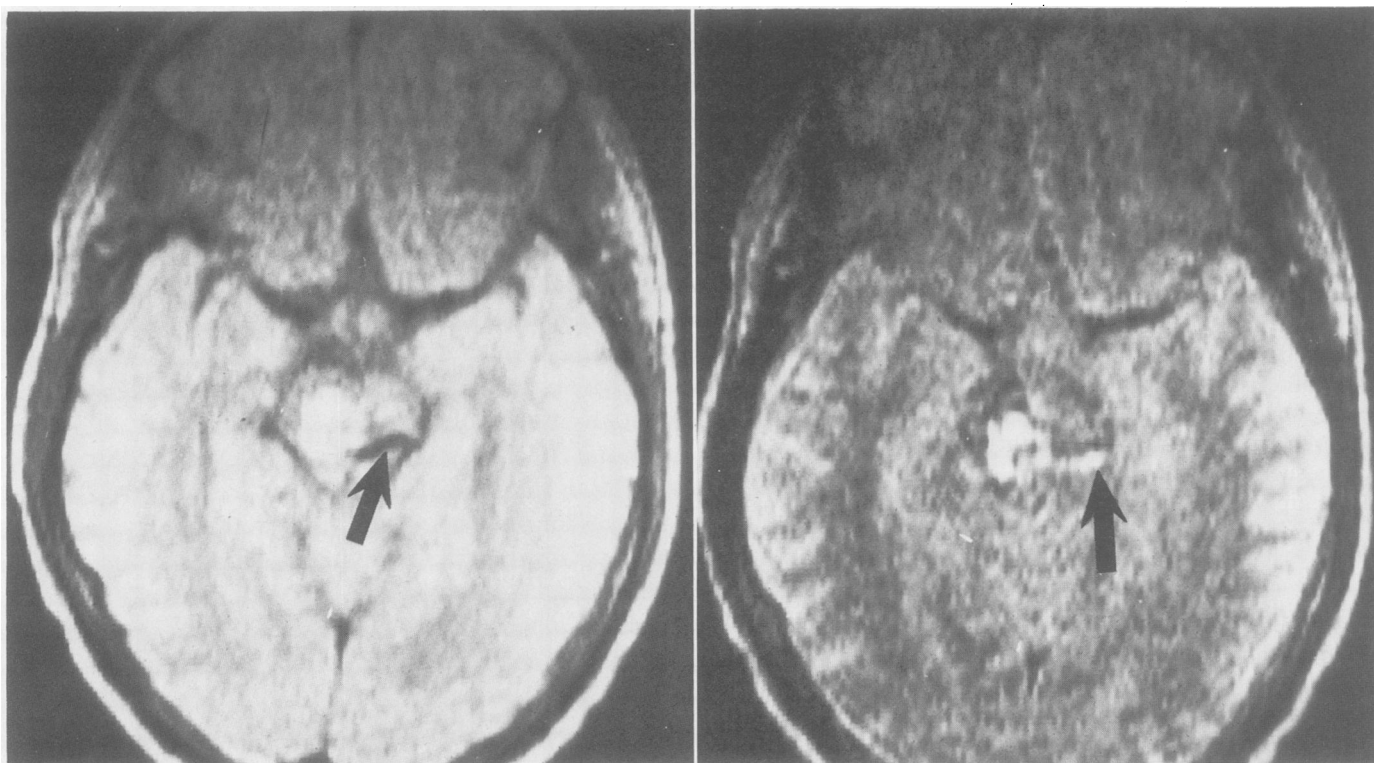


**Figure 3.**—Even-echo rephasing phenomenon on magnetic resonance imaging. A hemorrhagic arteriovenous malformation involving the right cerebral peduncle is shown by a multiecho sequence. The draining vein is dark on the first echo (left arrow) and bright on the second echo (right arrow).

An arteriovenous malformation has slow venous flow; hence, a multiecho sequence displaying increased signal intensity during each even echo is often taken as diagnostic for an arteriovenous malformation.<sup>13,14</sup> Waluch and Bradley have termed this phenomenon "even-echo rephasing in slow laminar flow" (Figure 3).<sup>15</sup> Three factors contribute to this phenomenon: the slow laminar flow in a vessel, the gradient present in the magnetic field and the spin-echo technique used. Following the 90° pulse, the signal produced after the first 180° pulse (odd echo) is weak because the spins have not completely rephased. The signal produced after the second 180° pulse (even echo) is stronger because the spins have completely rephased. Hemorrhagic arteriovenous malformations display a high signal intensity in a T1-weighted scan after a few days.

#### *Sellar and Parasellar Regions*

In the sellar and parasellar regions, one principal advantage of MR imaging is its lack of bone artifacts. Mark and colleagues<sup>16</sup> have reported that the pituitary yields a moderate signal, similar to that from the pons. A low signal from the pituitary may reflect partial volume averaging with vascular channels lateral to the gland. The high signal intensity near the posterior and inferior regions of the gland is contributed by fatty marrow in the posterior clinoid processes. A small fat pad is also present in the posteroinferior aspect of the sella.<sup>16</sup> The lamina dura defining the pituitary inferiorly yields no MR imaging signal and appears dark when the sphenoid sinus is incompletely pneumatized. With thinner slices and better spatial resolution, MR imaging should become the first investigative procedure when a pituitary tumor is suspected. Involvement of the optic tract and the optic chiasm and the suprasellar extent of the tumor can be appreciated on sagittal T1 images. Chromophobe and prolactin adenomas have long T1 and T2 relaxation times and therefore appear dark on T1-weighted images and bright on T2-weighted images. Craniopharyngioma is better evaluated by CT because calcifications, which are important for the diagnosis, do not return an MR imaging signal.

#### *Craniocervical Junction*

Magnetic resonance imaging depicts the craniocervical junction with considerable definition. Sagittal views provide direct visualization of the brain stem, cerebellar tonsils and upper cervical spine, with a resolution significantly superior to that of reformatted sagittal CT views. Abnormal conditions visible on MR images include basilar invagination due to conditions such as rheumatoid arthritis and Paget's disease, tumors such as clival meningiomas and brain-stem gliomas, basilar tip aneurysms, arachnoid cysts, Arnold-Chiari malformations and syringomyelia.

#### *Spine*

Magnetic resonance imaging is rapidly becoming the preferred method for examining the spinal canal and cord. A short spin-echo technique yields sharp contrast between the spinal cord and the subarachnoid space; cortical bone and CSF are not separable, however. Vertebral bodies yield a strong signal because of the presence of marrow, with its short T1 time. A long spin-echo technique emphasizes T2 and increases the signal from the normal nucleus pulposus and CSF.

With a long echo time (120 ms) and a long repetition time (2,000 ms), one can obtain images with contrast comparable with that of a myelogram.<sup>17</sup>

*Extradural lesions.* Disk degeneration is usually identified in an earlier stage by MR imaging than by CT<sup>17</sup>; small and lateral herniations, however, are sometimes diagnosed better with CT.<sup>17</sup> T2-weighted images separate the normal nucleus pulposus from the annulus and degenerated disk and permit identification of medial disk herniation and canal stenosis (Figure 4).<sup>17</sup>

In the vertebral disk in the young, MR imaging can differentiate between nucleus pulposus and annulus because they have a different water content. This difference decreases with age, leading to a diminution in the signal difference between the two structures.

MR imaging is as accurate as CT and myelography in the depiction of canal stenosis and shows the caudal and cranial extent of the stenosis in the case of complete block.<sup>17</sup>

Neoplasms involving the vertebral bodies yield a reduced signal in T1-weighted images and an increased signal in T2-weighted images.<sup>17</sup> These properties permit a clinician to differentiate between degenerative changes and metastases in some cases. Because of blood flow, hemangiomas usually remain dark in both T1- and T2-weighted sequences. If the flow rate is slow enough, however, hemangiomas can yield high signal intensity in T1-weighted images.

In irradiated vertebrae, fatty degeneration yields an increased signal in T1-weighted images (Figure 5).

Magnetic resonance imaging is an excellent modality for evaluating fractures that may encroach on the subarachnoid



**Figure 4.**—Multiecho sequence (echo time, 30 and 60 ms; pulse repetition time, 1,500 ms). A central bulging disk at L5-S1 is pushing on the prevertebral fat.



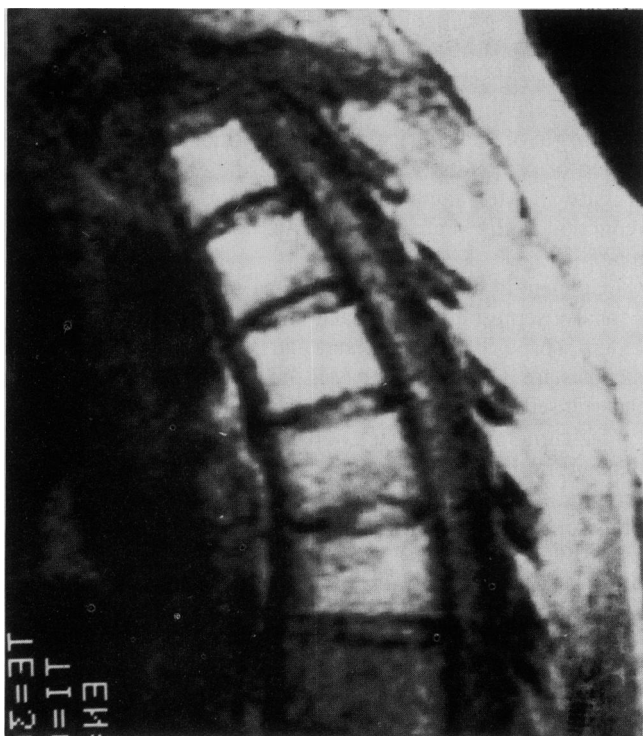


**Figure 5.**—Fatty degeneration after radiation therapy. A spin-echo sequence using an echo time of 30 ms and a pulse repetition time of 500 ms yields increased signal from several vertebral bodies with fatty replacement of the normal bone marrow after radiation therapy.

space and cord. Although bone fragments do not return a signal, acute secondary hemorrhage within the spinal canal and neural foramina follows the pattern of extravascular blood elsewhere and can be evaluated.

For a display of infection, MR imaging is more sensitive than plain films or CT and as sensitive as and more specific than radionuclide studies.<sup>17</sup> Diskitis is characterized by increased T1 and T2 times and involves the disk and the endplates. Degenerative changes have a short T2.<sup>17</sup>

For evaluation of subluxation, sagittal views can be taken in extension and flexion. This relatively dynamic study shows the relationship between the cord and bony structures and is particularly useful for diagnosing C-1 and C-2 subluxation, rheumatoid arthritis, basilar invagination and postoperative bony fusions.

**Intradural lesions.** Lipomeningoceles are displayed well with MR imaging because lipomas yield a very strong signal in T1-weighted images. This condition is often associated with a tethered cord, which is also easily depicted.<sup>18</sup> Meningiomas have a long T1 and a variable T2; compression of the cord by these tumors is shown well with MR imaging. Lymphomas have long T1 and T2 times. Because of this, the margins of the cord often are not well delineated on T1-weighted images. Metastases have long T1 and long T2 times, with the exception of melanoma metastases. These may yield a high signal intensity on T1-weighted images because they are hemorrhagic or contain melanin (which is paramagnetic), or both. Many primary tumors have long T1 and T2 relax-

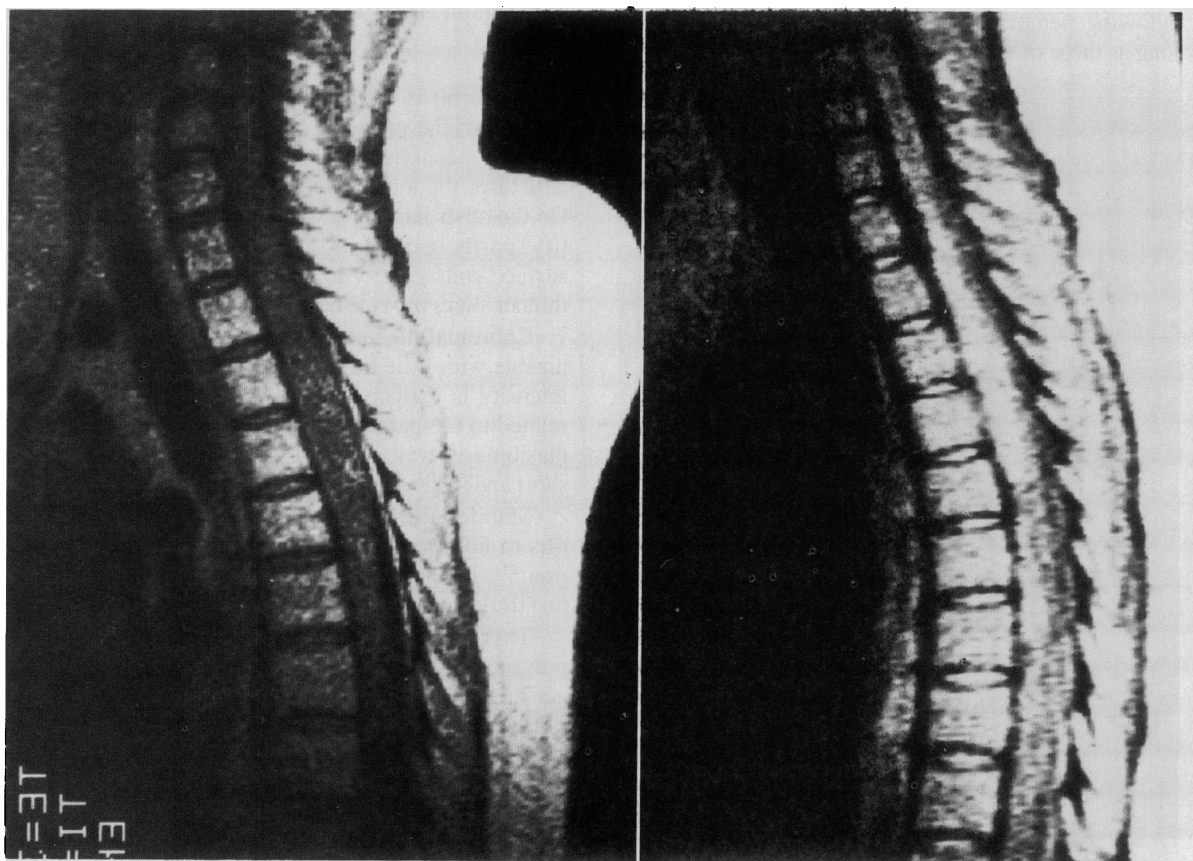


**Figure 6.**—Cord tumor. **Left,** A T1-weighted image (echo time [TE], 30 ms; repetition time [TR], 500 ms) using a spine surface coil. The cord is enlarged. **Right,** In a T2-weighted scan (TE, 75 ms; TR, 1,500 ms), the cord has an abnormally intense signal because of the prolonged T2 of the tumor.

ation times, yielding a high signal intensity on T2-weighted scans. Often the tumor enlarges the cord, a finding best depicted on T1-weighted scans (Figure 6).

Magnetic resonance imaging is an accurate and sensitive method for detecting cystic cavities such as those of syringomyelia, hydromyelia and progressive posttraumatic cystic myelopathy. On T1-weighted scans the cavity appears as a region of decreased signal, identical to that of the CSF. On T2-weighted images the adjacent cord might have an increased signal intensity as a result of myelomalacia.

Demyelinating diseases such as multiple sclerosis yield an increased signal intensity when a long spin-echo technique is used; the increase is caused by the prolonged T2 of the abnormal areas. MR imaging is a very sensitive technique for depicting these conditions.

With MR imaging, a divided spinal cord (diastematomyelia) is well imaged over its entire craniocaudal extent. When the bony septum contains marrow, it also is visible.<sup>19</sup>

### *Pediatric Applications*

Magnetic resonance imaging is a sensitive technique for detecting deficient or delayed myelination of the brain in children. Inversion recovery seems to be the most sensitive technique because it optimizes the contrast between grey and white matter.<sup>20</sup>

Parenchymal and subependymal hemorrhages are easy to recognize 48 hours after they occur because they yield an intense signal on a T1-weighted scan. Before 48 hours they have long T1 and T2 times.<sup>20</sup> Porencephalic cysts, a late finding following hemorrhage, have T1 and T2 relaxation times as long as those of ventricular CSF if the cyst communi-

cates with the arachnoid space, thereby permitting differentiation of this condition from acute hemorrhage.

Hydrocephalus is easy to detect on a T1-weighted scan. If it is obstructive, it is accompanied by transependymal flow at the margin of the ventricular system, which is visualized as a region of prolonged T2 surrounding the enlarged ventricles (Figure 7). After shunt placement, MR imaging often shows a reduction in the ventricular size and in the surrounding edema.<sup>20</sup>

Congenital abnormalities such as semilobar holoprosencephaly, septo-optic dysplasia, absence of the septum pellucidum, corpus callosum aplasia and dysplasia and aqueductal stenosis are detectable with MR imaging after the fontanelles have closed and ultrasonography is no longer useful.<sup>20</sup>

Ischemic anoxic encephalopathy with extensive areas of damage in the white matter is depicted by MR imaging. In neonatal hypoxia, phosphorus spectroscopy can show cerebral ischemia before this condition is detectable with ultrasound or CT studies.<sup>21</sup>

Cerebral palsy yields an increased signal in the anterior periventricular regions.<sup>20</sup>

## **Head**

### *Temporomandibular Joint*

The main advantage of MR imaging of the temporomandibular joint is its provision of sagittal and coronal views and its superb soft tissue contrast. Its ability to image the disk and surrounding tissues is particularly useful.<sup>22</sup> The use of surface coils and thin slices may facilitate replacement of CT and arthrography by MR imaging.<sup>22</sup>

### *Orbit*

The orbit is well suited to examination by MR imaging because of the presence of retrobulbar fat. Because the MR imaging signal depends on the water and protein content of a structure, the lens is well differentiated from vitreous fluid. On the other hand, the sclera and cornea are difficult to identify, partly because of the motion of the globe.<sup>23</sup> The use of surface coils greatly improves the signal-to-noise ratio, and thinner slices provide better spatial resolution.<sup>24</sup>

Choroidal melanoma yields a strong signal and is recognizable with little difficulty by MR imaging. The high signal intensity is explained by a short T1 relaxation time that is related to the paramagnetic properties of melanin.<sup>23</sup> Retinoblastoma is well shown by spin-echo sequences with both short and long repetition times.<sup>24</sup>

Manifestations of orbital pseudotumor vary from vasculitis to fibrotic sclerosis to generalized lymphocytic infiltration.<sup>23</sup> The increased water content lengthens the T1 time so that the lesion appears dark on T1-weighted scans.

Thyroid ophthalmopathy is caused by deposition of mucopolysaccharides, infiltration of plasma cells and lymphocytes and an increase in the orbital connective tissue.<sup>23</sup> In this condition the T1 and T2 values are prolonged in contrast to the short T1 of fat.

Most tumors involving the lacrimal fossa, such as adenoid cystic carcinoma, metastatic adenocarcinoma and lymphoma, have prolonged relaxation values, making them indistinguishable from each other by MR imaging.<sup>24</sup> A dermoid tumor from a patient in the series reported by Sobel and associates<sup>24</sup> had a short T1 because of the presence of fat, and a more



**Figure 7.**—Obstructive hydrocephalus due to a colloid cyst of the third ventricle. A T2-weighted scan shows abnormal signals surrounding the ventricles as a result of transependymal flow of cerebrospinal fluid.

specific diagnosis could be made. With thinner slices and surface coils for the orbit, MR imaging should become very useful in distinguishing optic nerve gliomas and neuritis. The ability of MR imaging to differentiate normal and pathologic orbital tissue is equal to that of CT.<sup>23</sup> However, MR imaging is more sensitive than CT in depicting intraorbital hemorrhage and ischemia of the globe.<sup>25</sup>

### *Nasopharynx*

Tumors producing mass effects are well delineated by MR imaging because of the displacement of fat in the nasopharynx. A long repetition time (T2-weighted scan) is usually used to differentiate muscle from tumor and to enhance visualization of the tumor. Detection of adenopathy is important for defining nasopharyngeal carcinoma; MR imaging can clearly differentiate adenopathy from muscle because involved lymph nodes produce a stronger signal. The retropharyngeal space lies between the pharyngobasilar and prevertebral fasciae; in normal conditions it is not visible either by MR imaging or CT. In pathologic conditions such as nasopharyngeal carcinoma, adenopathy can be detected in this region.<sup>26</sup>

The base of the skull requires careful analysis because tumor usually grows upward along fascial planes in the nasopharynx to this region. Sagittal MR imaging views show tumor extension through the clivus and depict involvement of the sphenoid sinus (Figure 8). The clivus produces a strong signal on all pulse sequences because of its marrow content. The sphenoid sinus has no signal because of its aeration; therefore, inflammation and tumor extension are well depicted by MR imaging. Dysfunction of the eustachian tube, otitis media or mastoiditis on the ipsilateral side is often associated with neoplastic processes of the nasopharynx. These lesions produce an intense signal that is easy to recognize in transverse views.

### *Salivary Glands*

Parotid tumors (adenocystic carcinoma and sarcoma) and submandibular gland carcinomas have prolonged T1 and T2 values that are different from normal glandular tissue and adjacent muscles and fat.

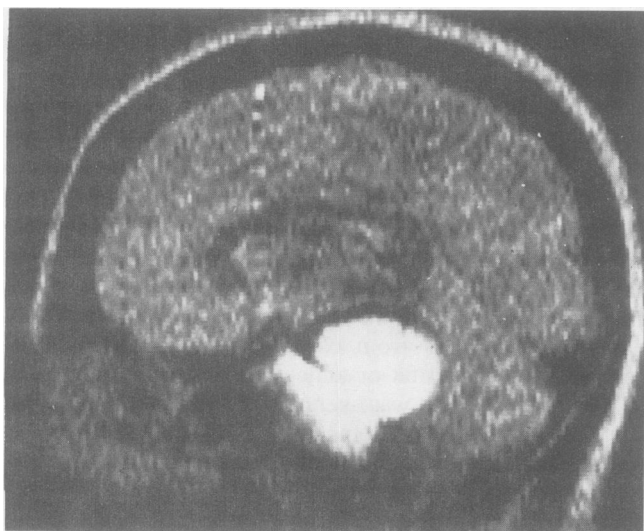


**Figure 8.**—A T2-weighted scan shows a chordoma involving the clivus and extending to the posterior fossa.

### **Neck**

Although the spatial resolution of MR imaging is slightly inferior to that of high-resolution CT,<sup>27</sup> the greater contrast resolution of MR imaging and its flexibility with regard to transaxial, coronal and sagittal imaging permit excellent differentiation of normal tissues, tumors, lymph nodes, muscles and blood vessels.<sup>27</sup> Elliptical radio-frequency coils can be used to increase the signal-to-noise ratio when this anatomic region is imaged with magnetic resonance.

Thyroid nodules, cysts and normal tissue usually can be differentiated in MR images.<sup>28</sup> Thyroid cysts have the greatest water content and the longest T1 and T2 relaxation times.<sup>28</sup> Parathyroid adenomas may have slightly longer relaxation times than those of a hyperplastic parathyroid gland; this finding has not been confirmed in duplicated studies, however.<sup>28</sup>

Generally, abnormal lymph nodes have increased T1 and T2 times. MR imaging has advantages over CT in differentiating enlarged lymph nodes from muscles and from tortuous vessels in the neck.<sup>28</sup> The signal intensity of scar tissue does not increase significantly when the repetition time is increased; consequently the T2 time of scar tissue appears to be short relative to other tissues and to recurrent tumor.<sup>28</sup> Tumors involving the laryngeal tract and their extension into the parapharyngeal space are well depicted by MR imaging.

### **Mediastinum and Chest**

It is relatively easy with MR imaging to differentiate masses (either adenopathy or extension of bronchogenic carcinoma) from vascular structures in the chest because flowing blood provides high intrinsic contrast. To differentiate mediastinal fat from tumor, T1-weighted images are used. In these images, the tumor mass will be dark (a long T1 time) and the fat will be bright (a short T1 time). Because of overlapping relaxation times, T1 and T2 computations do not permit differentiation of sarcoidosis from lymphoma.<sup>29</sup> MR imaging depicts enlarged tortuous vessels without difficulty.

Compared with CT, MR imaging has inferior spatial resolution because it uses thicker slices and is more vulnerable to cardiac and respiratory motion. Cardiac gating improves resolution but increases scan duration. Nevertheless, in many cases MR imaging shows differences between small vessels and abnormal nodules better than does CT. In the future, MR imaging may permit quantification of lung fluid, making it useful in the management of pulmonary edema and hemorrhage.<sup>30</sup> Early experimental work suggests that MR imaging may be useful in showing distal pulmonary emboli (high signal intensity on T1-weighted images). Proximal pulmonary emboli sometimes are misinterpreted as mediastinal fat.<sup>31</sup>

Magnetic resonance imaging has considerable potential for detecting pulmonary diseases in children. On chest roentgenograms it can be difficult to differentiate normal pulmonary vessels from adjacent linear atelectasis, bronchi with mucoid impaction and peribronchial inflammatory changes. This problem led Gooding and associates to compare MR imaging with CT and chest roentgenography in six children with cystic fibrosis.<sup>32</sup> More mucoid plugs were evident with MR imaging than with chest roentgenography, and more mediastinal nodes were apparent with MR imaging than with CT. In children with cystic fibrosis, MR imaging showed a

shrunk pancreas that yields a strong signal as a result of fatty replacement.<sup>32</sup> Gooding and co-workers suggest that MR imaging may become the principal imaging modality in patients suspected to have cystic fibrosis.<sup>32</sup>

### Cardiovascular Systems

Ungated cardiac images are subject to considerable resolution loss due to motion; the images are improved significantly by gating. Cardiac images with excellent spatial resolution can be obtained by gating at various times within the cardiac cycle, at the expense of a slight increase in imaging time. In the case of septal defects, atrioventricular canal defects are shown well by MR imaging, as are ventricular septal defects. MR imaging permits assessment of atrioventricular valve morphology, chamber sizes and ventricular wall thickness.<sup>33</sup> Ventricular hypoplasia is well depicted, and signal analysis of the myocardium can be helpful in showing fatty replacement. T1-weighted scans are the most widely used gated cardiac images.<sup>33</sup>

Various valvular diseases are successfully shown by MR imaging. In aortic stenosis, for instance, valves appear thicker and have decreased mobility; they sometimes are visible in systole, whereas normal valves are not visible in this phase. Great vessel abnormalities are often recognizable (Figure 9), although identification of specific structures is sometimes difficult.<sup>33</sup> Palliative systemic pulmonary artery shunt normally is free of signal, indicating flowing blood. A clot in the shunt appears bright, as does turbulent and slowly flowing blood.

MR imaging may show the presence of myocardial infarction because the signal intensity of the infarcted region is

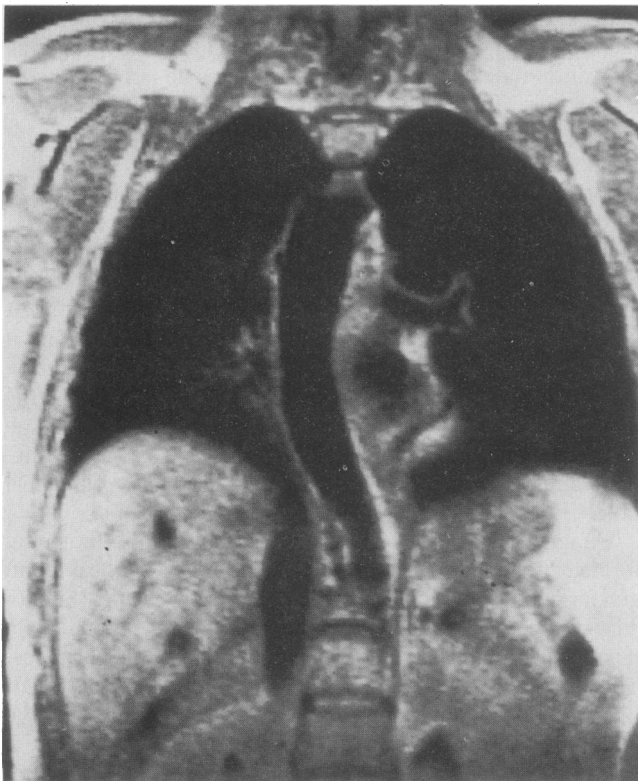


**Figure 9.**—A gated cardiac scan, coronal view, depicting a right descending aorta.

higher (prolonged T2 time) than that of the surrounding normal myocardium.<sup>34</sup> Magnetic resonance spectroscopy of endogenous phosphates in the myocardium may eventually permit assessment of the functional integrity of myocardium.<sup>35</sup> Paramagnetic intravenously administered contrast agents that shorten T1 and T2 relaxation times could be useful for early detection of myocardial ischemia in the future. Manganese ions (<sup>52</sup>Mn and <sup>54</sup>Mn) are distributed in the myocardium in proportion to blood flow. Consequently, ischemic myocardial regions show a deficiency in Mn<sup>++</sup> distribution.<sup>35</sup> In patients with cardiac failure, slowly flowing blood in the ventricle produces a high signal intensity. Ventricular aneurysms are also shown by slow and turbulent blood flow and by thinning and bulging of affected cardiac wall.

Magnetic resonance imaging promises to become an important modality for evaluating pericardial disease. It can differentiate simple pericardial cysts from pericardial masses, fat and diaphragmatic eventration.<sup>36</sup> MR imaging shows normal pericardium as a 1- to 2-mm thick curvilinear structure of low signal intensity.<sup>36</sup> Changes in this configuration occur in constrictive pericarditis, inflammations and effusions.

Cardiac tumors are identifiable as thickening of the chamber wall, with decreased systolic ejection volume and abnormal signal intensity from the tumor.

The contrast between flowing blood and vessel wall permits evaluation of several vascular diseases. The signal from flowing blood is highly dependent on the pulse sequence and pulsing times chosen for the study. Atherosclerotic plaques are dark when they contain connective tissue, and they are surrounded by high signal intensity caused by lipid accumulation. Calcifications are frequently not detected as they produce no signal.<sup>37</sup>

Magnetic resonance imaging can show aneurysms and aortic dissections without a contrast agent. Coronal and sagittal views show the extent of these conditions and whether they involve the renal arteries. True and false channels are recognizable. Thrombus, slow laminar flow and turbulent flow can all produce increased signal and may be difficult to differentiate from each other. Because the MR imaging signal depends on flow velocity, there is considerable interest in calculating flow velocities from MR measurements.

### Breast

The breast is a heterogeneous organ composed of fat, epithelial tissue and fibrous stroma in different proportions. Fat is readily differentiated from other tissues by MR imaging and produces a strong signal because of its short T1 time. The T1 time of ducts and fibrous stroma varies with the menstrual cycle and with the use of exogenous hormones. Age and pregnancy also affect the T1 value. In a study by McSweeney and associates, discrimination based on T2 values could differentiate benign lesions from carcinoma in specimens that contained tumor and fat or tumor and a mixture of fat and fibrous tissue.<sup>38</sup> There was overlap of T2 values in specimens containing tumor and predominantly fibrous tissue. Cysts are well visualized, but calcifications are not seen. Paramagnetic contrast agents conjugated with specific monoclonal antibodies are being investigated in an effort to increase the sensitivity and specificity of MR imaging for breast cancer detection. MR imaging may be useful in staging breast tumors



because of its ability to detect axillary and supraclavicular adenopathy and chest wall involvement by tumor.

## Abdomen

Respiratory gating of abdominal MR imaging scans has improved spatial resolution in some cases. In this process, information is acquired only between the end of expiration and the beginning of inspiration, so that motion artifacts are reduced. Scan time is significantly increased, however.

Magnetic resonance imaging is very sensitive to liver disease. However, the signal intensity of tumors varies strongly with the pulse sequence used.<sup>39</sup> The T1 and T2 values of different liver tumors extend over a rather narrow range, and MR imaging has difficulty differentiating between benign and malignant processes. Paramagnetic agents could help increase MR imaging sensitivity dramatically for liver disease. MR imaging appears to be more definitive than CT in showing the internal architecture of a liver mass, its extent and its relationship with vascular structures.<sup>39</sup> Some authors have reported that T2 is longer for neoplastic processes than for normal liver and that pulse sequences which emphasize differences in T2 values might show liver lesions earlier.<sup>40</sup> With the development of spectroscopy, magnetic resonance could gain greater specificity by identifying metabolic changes in affected tissues.

In diffuse liver disease MR imaging has an important role. It detects hepatitis and cirrhosis because the T1 value of affected tissues is longer than that of normal liver. In hemosiderosis and hemochromatosis, the T1 value is decreased due to the presence of paramagnetic iron deposits.<sup>41,42</sup>

The pancreas is difficult to image with any imaging modality, including magnetic resonance. One advantage of MR imaging is the lack of bone- or gas-induced artifact. Smith has reported that differences in the T1 of normal and cancerous pancreas may give MR imaging an advantage over ultrasound, CT and nuclear medicine.<sup>43</sup> Margins of pancreatic pseudocysts are often shown better by CT than by MR imaging.<sup>44</sup>

Transverse and coronal views nicely show both kidneys. T1-weighted inversion recovery images yield excellent corticomedullary differentiation.<sup>45</sup> Cortex and columns of Bertin are light-grey because of their relatively short T1 value, whereas the medulla is dark because of its longer T1 time. Perirenal fat provides a strong signal that delineates both kidneys and permits evaluation of the extracapsular extension of a renal tumor. MR imaging is able to differentiate cystic from solid masses and to depict fatty components within the lesion. Tumor extension into or around renal veins and arteries, inferior vena cava and aorta is best evaluated using transverse and sagittal views.

Renal failure is accompanied by a loss of corticomedullary differentiation. This observation is helpful in evaluating renal function. The loss of corticomedullary differentiation is also seen in acute and chronic rejection. However, acute rejection is accompanied by a low signal intensity from the transplanted kidney.<sup>46</sup> In acute tubular necrosis the corticomedullary differentiation is variable.<sup>46</sup>

Magnetic resonance imaging is sometimes helpful in detecting abnormal adrenals; in general, however, there appears to be no significant improvement over CT.<sup>47</sup> Although small calcifications are not detected, MR imaging is useful for visu-

alization of adjacent major vascular structures.<sup>47</sup> In some cases, adrenal hyperplasia is shown as an inner region of low intensity surrounded by an outer region of higher intensity.<sup>47</sup>

In children, abdominal masses present a diagnostic challenge. MR imaging shows tumor spread to bone marrow, liver and abdominal lymph nodes and demonstrates vessel encasement, the major factor limiting surgical resection.<sup>48</sup> In children with neuroblastoma, Cohen and colleagues found MR imaging to be very helpful in showing metastatic disease and in aiding the prediction of tumor resectability.<sup>48</sup> Neuroblastoma shows prolonged T1 and T2 times. On a T1-weighted scan, therefore, neuroblastoma appears darker than adjacent liver and muscle, whereas on a T2-weighted scan the tumor signal is increased. MR imaging can be used to monitor the response of neuroblastoma to chemotherapy and radiation therapy.<sup>48</sup> A major disadvantage of MR imaging is that calcifications are not seen. This limitation makes it difficult to differentiate neuroblastoma from Wilms' tumor.

## Pelvis

The pelvis is depicted well by MR imaging because of the high level of contrast provided by pelvic fat, urine in the bladder and gas in the bowel. There is little blurring caused by motion, and the large amount of bone in this region does not interfere with MR imaging.<sup>49,50</sup> Images are acquired in transverse, coronal and sagittal planes. In a spin-echo sequence, the uterus, prostate and seminal vesicles have a slightly higher signal intensity than do the skeletal muscles.<sup>50</sup>

For a clear distinction of ovary from surrounding adipose tissue, a short spin-echo technique is preferred.<sup>51</sup> Ovarian cysts yield variable signal intensities that depend on their protein and cholesterol content.<sup>50</sup> Unfortunately, some large serous cystadenomas have the same signal intensity as urine. In papillary cystadenofibroma, the cystic portion yields an intense spin-echo signal, indicating a long T1 time, whereas the solid portion has the appearance of muscle (dark).<sup>52</sup> Dermoid tumors contain considerable fat and yield a high signal intensity in all sequences because of a short T1 and moderate T2 value. Some areas may remain dark because of the presence of calcific material.

Sagittal as well as transverse images are used to show the uterus.<sup>50</sup> The endometrium yields a stronger MR imaging signal than does the myometrium, which in turn is slightly stronger than the striated muscle of the pelvic wall. The myometrium and endometrium are separated by a low signal line, probably the stratum basale.<sup>51</sup> The endocervix may have a high signal intensity because of the presence of mucus.<sup>51</sup> Leiomyomas are differentiated from normal uterus by increases in both T1 and T2 times and by their presentation as homogeneous masses. With a short spin-echo technique, endometriosis may provide an increased signal intensity due to the presence of hemorrhage.<sup>52</sup> Endometrial carcinoma has prolonged T1 and T2 relaxation times and appears as an inhomogeneous mass because of necrotic areas.<sup>50</sup>

The vagina usually provides a weaker signal than does the uterus.<sup>51</sup> MR imaging provides important information regarding the anatomic relationship of the vagina, bladder and rectum.

The normal prostate gland is homogeneous and has a medium signal intensity, which increases slowly as the repetition time increases.<sup>53</sup> Calcifications yield no signal. Benign hy-

peritrophy of the gland has a tendency to elevate the floor of the bladder; this is best shown on coronal or sagittal images.<sup>50</sup> Prostatic carcinoma is presented as an inhomogeneous mass.<sup>54,55</sup> When a short spin-echo sequence is used, malignant nodules yield a weaker signal than does the normal gland. A strong signal is sometimes present as a result of intratumoral hemorrhage.<sup>53</sup> Tumor extension is apparent because the normal gland is surrounded by a pencil-thin rim of lower intensity and by pelvic fat in the space of Retzius. This fat can be distinguished easily from the pelvic prostatic ligament.<sup>53</sup> The prostate, rectum and levator ani muscles are all easily distinguished. Because the seminal vesicles are bright in a long spin-echo sequence, their gross involvement in prostatic cancer is easy to detect.<sup>53</sup> Prostatitis and carcinoma have overlapping relaxation times.<sup>54</sup>

Magnetic resonance imaging is an excellent method for investigating bladder disease. The urine in and the fat surrounding the bladder permit clear delineation of this structure. Normal bladder wall is thin and identifiable as a discrete structure.<sup>50</sup> Wall thickening by chronic obstruction is readily detected, as is carcinoma, which produces a bright signal when a long pulse sequence is used. Extravesical extension into the perivesical fat is generally more obvious with MR imaging than with CT.<sup>56</sup> MR imaging has already assumed a prominent role in the clinical evaluation of carcinoma of the bladder and prostate.<sup>53</sup>

### Musculoskeletal System

Magnetic resonance imaging is the method of choice in the diagnosis of avascular necrosis of the femoral head. In their comparative study of 38 healthy subjects and 20 patients with abnormalities, Totty and associates showed that MR imaging was superior to both roentgenography and scintigraphy in depicting this condition.<sup>57</sup> The normal femoral head is surrounded by a thin low-intensity cortex. With all pulse sequences, the medullary cavity has a strong signal intensity emanating from the large deposits of fat and from hematopoietic cells. Regions of reduced intensity crossing the high-intensity cavity are due to the physis (transversally oriented) and the weight-bearing trabeculae (vertically oriented). Between 12 and 48 hours after an ischemic insult, the signal becomes very low because of the death of osteocytes, hematopoietic cells and, eventually, fat cells in the infarcted region.<sup>57</sup>

Magnetic resonance imaging can be used to evaluate ligamentous tears after acute knee injury. Sagittal and parasagittal views show the cruciate ligaments, and coronal views show the tibial and fibular collateral ligaments. On T2-weighted images, high signal intensity between the medial collateral ligament and the medial meniscus is considered diagnostic of a torn medial collateral ligament.<sup>58</sup>

Because of its exquisite soft tissue differentiation, MR imaging can be used to detect bone tumors and to evaluate the extension of the tumor into adjacent soft tissue and bone marrow. MR imaging provides high-resolution images of extremities and shows tumor by changes in both anatomic structure and relaxation time.<sup>59</sup>

### Conclusion

Magnetic resonance imaging is already an important and useful clinical tool because it uses no ionizing radiation. Its

safety and sensitivity suggest that it may replace many invasive and risky techniques such as myelography. This new imaging modality has become competitive with computed tomography. The use of paramagnetic contrast agents, thinner slices and surface coils will add more specificity and will provide better spatial resolution. Spectroscopy promises detection of early pathologic changes in metabolism.

### REFERENCES

1. Buonanno FS, Kistler JP, DeWitt LD, et al: Nuclear magnetic resonance imaging in central nervous system disease. *Semin Nucl Med* 1983 Oct; 13:329-337
2. Lee BCP, Kneeland JB, Walker RW, et al: MR imaging of brainstem tumors. *AJNR* 1985 Mar/Apr; 6:159-163
3. Brant-Zawadzki M, Badami JP, Mills CM, et al: Primary intracranial tumor imaging: A comparison of magnetic resonance and CT. *Radiology* 1984 Feb; 150:435-440
4. Kingsley DPE, Brooks GB, Leung AWL, et al: Acoustic neuromas: Evaluation by magnetic resonance imaging. *AJNR* 1985 Jan/Feb; 6:1-5
5. Zimmerman RD, Fleming CA, Saint-Louis LA, et al: Magnetic resonance imaging of meningiomas. *AJNR* 1985 Mar/Apr; 6:149-157
6. Horvath K, Fink I, Patronas NJ, et al: MR characterization of neurofibromas and neurofibrosarcomas. Presented at the 70th Scientific Assembly and Annual Meeting of the Radiological Society of North America, Washington, DC, November 1984
7. Jackson JA, Leake DR, Schneiders NJ, et al: Magnetic resonance imaging in multiple sclerosis: Results in 32 cases. *AJNR* 1985 Mar/Apr; 6:171-176
8. Aisen AM, Gabrielson TO, McCune WJ: MR imaging of systemic lupus erythematosus involving the brain. *AJNR* 1985 Mar/Apr; 6:197-201
9. Gandy SE, Snow RB, Zimmerman RD, et al: Cranial nuclear magnetic resonance imaging in head trauma. *Ann Neurol* 1984 Aug; 16:254-257
10. Bradley WG Jr: Magnetic resonance imaging of the central nervous system. *Neurol Res* 1984 Sep; 6:91-106
11. Sipponen JT, Sepponen RA, Sivula A: Nuclear magnetic resonance (NMR) imaging of intracerebral hemorrhage in the acute and resolving phases. *J Comput Assist Tomogr* 1983 Dec; 7:954-959
12. Flannigan BD, Bradley WG, Kortman KE: Evolution of cerebral infarction: MRI appearance with pathophysiological correlation. Presented at the Society for Magnetic Resonance Meeting, 3rd Annual Meeting, San Diego, Mar 1985
13. Bradley WG Jr, Waluch V: Blood flow: Magnetic resonance imaging. *Radiology* 1985 Feb; 154:443-450
14. Bradley WG Jr, Waluch V, Lai KS, et al: The appearance of rapidly flowing blood on magnetic resonance images. *AJR* 1984 Dec; 143:1167-1174
15. Waluch V, Bradley WG: NMR even echo rephasing in slow laminar flow. *J Comput Assist Tomogr* 1984 Aug; 8:594-598
16. Mark L, Pech P, Daniels D, et al: The pituitary fossa: A correlative anatomic and MR study. *Radiology* 1984 May; 153:453-457
17. Modic MT, Hardy RW Jr, Weinstein MA, et al: Nuclear magnetic resonance of the spine: Clinical potential and limitation. *Neurosurgery* 1984 Oct; 15:583-592
18. Modic MT, Weinstein MA, Pavlicek W, et al: Nuclear magnetic resonance imaging of the spine. *Radiology* 1983 Sep; 148:757-762
19. Han JS, Benson JE, Kaufman B, et al: Demonstration of diastematomyelia and associated abnormalities with MR imaging. *AJNR* 1985 Mar/Apr; 6:215-219
20. Johnson MA, Pennock JM, Bydder GM, et al: Clinical NMR imaging of the brain in children: Normal and neurologic disease. *AJR* 1983 Nov; 141:1005-1018
21. Cady EB, Dawson MJ, Hope PL, et al: Non-invasive investigation of cerebral metabolism in newborn infants by phosphorus nuclear magnetic resonance spectroscopy. *Lancet* 1983 May 14; 1:1059-1062
22. Helms CA, Richardson ML, Moon KL, et al: Nuclear magnetic resonance imaging of the temporomandibular joint: Preliminary observations. *J Craniomandib Pract* 1984 Jun/Aug; 2:220-224
23. Sobel DF, Mills C, Char D, et al: NMR of the normal and pathologic eye and orbit. *AJNR* 1984 Jul/Aug; 5:345-350
24. Sobel DF, Kelly W, Kjos BO, et al: MR imaging of orbital and ocular disease. *AJNR* 1985 Mar/Apr; 6:259-264
25. Edwards JH, Hyman RA, Vacirca SJ, et al: 0.6T magnetic resonance imaging of the orbit. *AJNR* 1985 Mar/Apr; 6:253-258
26. Dillon WP, Mills CM, Kjos B, et al: Magnetic resonance imaging of the nasopharynx. *Radiology* 1984 Sep; 152:731-738
27. Stark DD, Moss AA, Gamsu G, et al: Magnetic resonance imaging of the neck, Part I: Normal anatomy. *Radiology* 1984 Feb; 150:447-454
28. Stark DD, Moss AA, Gamsu G, et al: Magnetic resonance imaging of the neck, Part II: Pathologic findings. *Radiology* 1984 Feb; 150:455-461
29. Gamsu G, Webb WR, Sheldoh P, et al: Nuclear magnetic resonance imaging of the thorax. *Radiology* 1983 May; 147:473-480
30. Webb WR, Gamsu G: Clinical NMR imaging of the chest and mediastinum. *Diagn Imaging Clin Med* 1984; 53:22-28
31. Gamsu G, Hirji M, Moore EH, et al: Experimental pulmonary emboli detected using magnetic resonance. *Radiology* 1984 Nov; 153:467-470
32. Gooding CA, Lallemand DP, Brasch RC, et al: Magnetic resonance imaging in cystic fibrosis. *Pediatrics* 1984 Sep; 105:384-388
33. Jacobstein MD, Fletcher BD, Nelson AD, et al: ECG-gated nuclear magnetic resonance imaging: Appearance of the congenitally malformed heart. *Am Heart J* 1984 May; 107:1014-1020

# APPLICATION OF MAGNETIC RESONANCE IMAGING

34. Wesbey G, Higgins CB, Lanzer P, et al: Imaging and characterization of acute myocardial infarction in vivo by gated nuclear magnetic resonance. *Circulation* 1984 Jan; 69:125-130
35. Pohost GM, Ratner AV: Nuclear magnetic resonance: Potential applications in clinical cardiology. *JAMA* 1984 Mar; 251:1304-1309
36. Stark DD, Higgins CB, Lanzer P, et al: Magnetic resonance imaging of the pericardium: Normal and pathologic findings. *Radiology* 1984 Feb; 150:469-474
37. Herfkens RJ, Higgins CB, Hricak H, et al: Nuclear magnetic resonance imaging of atherosclerotic disease. *Radiology* 1983 Jul; 148:161-166
38. McSweeney MB, Small WC, Cerny V, et al: Magnetic resonance imaging in the diagnosis of breast disease: Use of transverse relaxation times. *Radiology* 1984 Dec; 153:741-744
39. Moss AA, Goldberg HI, Stark DB, et al: Hepatic tumors: Magnetic resonance and CT appearance. *Radiology* 1984 Jan; 150:141-147
40. Bernardino ME, Small W, Goldstein J, et al: Multiple NMR T2 relaxation values in human liver tissue. *AJR* 1983 Dec; 141:1203-1208
41. Doyle FH, Pennock JM, Banks LM, et al: Nuclear magnetic resonance imaging of the liver: Initial experience. *AJR* 1982 Feb; 138:193-200
42. Borkowski GP, Buonocore E, George CR, et al: Nuclear magnetic resonance (NMR) imaging in the evaluation of the liver: A preliminary experience. *J Comput Assist Tomogr* 1983 Oct; 7:768-774
43. Smith FW: Two years' clinical experience with NMR imaging. *Appl Radiol* 1983 May/Jun, pp 29-42
44. Davis PL, Moss AA, Goldberg HI, et al: Nuclear magnetic resonance imaging of the liver and pancreas. *RadioGraphics* 1984 Jan; 4:159-169
45. Steiner RE, Bydder GM: Nuclear magnetic resonance imaging of the abdomen. *Diagn Imaging Clin Med* 1984, pp 38-42
46. Geisinger MA, Risius B, Jordan ML, et al: Magnetic resonance imaging of renal transplants. *AJR* 1984 Dec; 143:1229-1234
47. Schultz CL, Haaga JR, Fletcher BD, et al: Magnetic resonance imaging of the adrenal glands: A comparison with computed tomography. *AJR* 1984 Dec; 143:1235-1240
48. Cohen MD, Weetman R, Provisor A, et al: Magnetic resonance imaging of neuroblastoma with a 0.15-T magnet. *AJR* 1984 Dec; 143:1241-1248
49. Baker HL, Berquist TH, Kispert DB, et al: Magnetic resonance imaging in a routine clinical setting. *Mayo Clin Proc* 1985 Feb; 60:75-90
50. Bryan PJ, Butler HE, LiPuma JP, et al: NMR scanning of the pelvis: Initial experience with a 0.3 T system. *AJR* 1983 Dec; 141:1111-1118
51. Hricak H, Alpers C, Cooks LE, et al: Magnetic resonance imaging of the female pelvis: Initial experience. *AJR* 1983 Dec; 141:1119-1128
52. Butler H, Bryan P, LiPuma JP, et al: Magnetic resonance imaging of the abnormal female pelvis. *AJR* 1984 Dec; 143:1259-1266
53. Hricak H, Williams RD, Spring DB, et al: Anatomy and pathology of the male pelvis by magnetic resonance imaging. *AJR* 1983 Dec; 141:1101-1110
54. Poon PY, McCallum RW, Henkelman MM, et al: Magnetic resonance imaging of the prostate. *Radiology* 1985 Jan; 154:143-149
55. Buonocore E, Hesemann C, Pavlicek W, et al: Clinical and in vitro magnetic resonance imaging of prostatic carcinoma. *AJR* 1984 Dec; 143:1267-1272
56. Resnick MI, Kursh ED, Bryan PD: Nuclear magnetic resonance imaging and bladder cancer. *Pathol Diagn Surg* 1984, pp 255-265
57. Totty WG, Murphy WA, Ganz WI, et al: Magnetic resonance imaging of the normal and ischemic femoral head. *AJR* 1984 Dec; 143:1273-1280
58. Turner DA, Prodromos CC, Petasnick JP, et al: Acute injury of the ligaments of the knee: Magnetic resonance evaluation. *Radiology* 1985 Mar; 154:717-722
59. Brady TJ, Gebhardt MC, Pykett IL, et al: NMR imaging of forearms in healthy volunteers and patients with giant-cell tumor of bone. *Radiology* 1982 Aug; 144:549-552